

A Facile Trans to Gauche Conversion in Layered Silver Butanethiolate

Hilary G. Fijolek, Jill R. Grohal, Jennifer L. Sample, and Michael J. Natan*

Department of Chemistry, 152 Davey Laboratory, The Pennsylvania State University, University Park, Pennsylvania 16802-6300

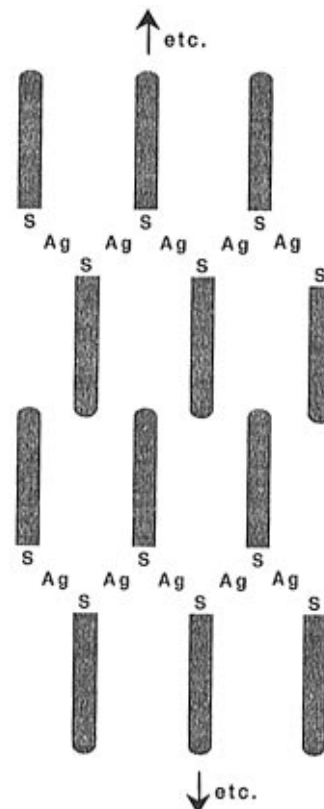
Received October 18, 1996[⊗]

Raman, X-ray diffraction (XRD), UV–visible reflectance, and ¹³C and ¹⁰⁹Ag CPMAS NMR studies have been carried out on three different forms of the layered solid AgS(CH₂)₃CH₃: a white all-trans compound, a bright yellow gauche C(1)–C(2) conformational isomer, and a phase containing both species. The structure of these compounds comprises a slab of Ag and S atoms, alkyl chains extending in both directions, and layer stacking. Raman spectroscopy and ¹³C NMR show that the all-trans species is less stable, converting cleanly to the gauche form. This transformation (*E*_a ≈ 60 kJ/mol) is accompanied by a color change from white to yellow, a phenomenon previously observed upon melting of mesogenic AgSR (R = alkyl) compounds. XRD shows that the 15.56 Å interlayer spacing in the trans form increases to 16.88 Å in the gauche form. On the basis of ¹⁰⁹Ag NMR data and bond lengths from structurally-characterized Ag thiolate model compounds, S–S spacings of 4.4–4.8 Å were found, which agree with those reported for two-dimensional self-assembled monolayers of organothiolates (SAMs) on well-defined Ag surfaces. These findings shed light on the molecular origins of AgSR mesogenic behavior and reinforce the idea that Ag–S interactions play a dominant role in self-assembly of organothiolates on Ag.

Introduction

Neutral, polycrystalline AgSR compounds [R = –(CH₂)_n–CH₃] have been described as layered solids with three key motifs:¹ (i) parallel slabs of connected Ag and S atoms with perpendicular alkyl chains extending in both directions; (ii) triply-bridging (μ₃-) S leading to three-coordinate Ag⁺ environments; and (iii) layer stacking based on van der Waals contact between all-trans alkyl chains that leads to interpenetration of methyl hydrogen atoms (Charts 1 and 2). These compounds exhibit thermotropic liquid crystalline behavior² and upon melting undergo bilayer to micellar structural rearrangements—unusual phenomena for covalent materials containing transition metals—that have been ascribed to a S μ₃-bridging → μ₂-bridging transition.³ In addition, aspects of AgSR structure are relevant to studies on two-dimensional (2-D) self-assembled monolayers (SAMs)⁴ formed by exposure of Ag to RSH.^{5,6} In contrast to the more widely-studied RS[–]/Au system,^{7–10} which adopts a (√3 × √3)R30° structure with fully

Chart 1. Layered Structure of AgS(CH₂)₃CH₃



extended, all-trans alkyl groups at an ≈30° tilt angle, RS[–] on Ag(111) exhibits a (√3 × √3)R10.9° lattice with tilt angles reported between 0 and 12°.⁵ This reconstruction derives from

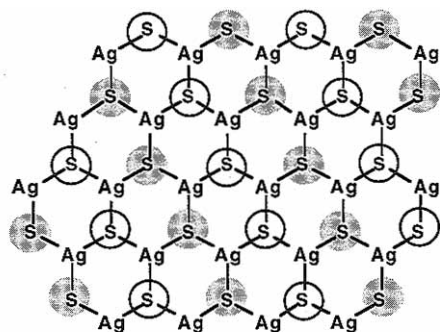
* Author to whom all correspondence should be addressed. Electronic mail: natan@chem.psu.edu.

[⊗] Abstract published in *Advance ACS Abstracts*, February 1, 1997.

- (1) Dance, I. G.; Fisher, K. J.; Banda, R. M. H.; Scudder, M. L. *Inorg. Chem.* **1991**, *30*, 183–187.
- (2) (a) Giroud-Godquin, A.-M.; Maitlis, P. M. *Angew. Chem., Int. Ed. Engl.* **1991**, *30*, 375–402. (b) Hudson, S. A.; Maitlis, P. M. *Chem. Rev.* **1993**, *93*, 861–885.
- (3) Baena, M. J.; Espinet, P.; Lequerica, M. C.; Levelut, A. M. *J. Am. Chem. Soc.* **1992**, *114*, 4182–4185.
- (4) (a) Ulman, A. *An Introduction to Ultrathin Organic Films: From Langmuir-Blodgett to Self-Assembly*; Academic Press, Inc: Boston, MA, 1991. (b) Bain, C. D.; Whitesides, G. M. *Angew. Chem., Int. Ed. Engl.* **1989**, *28*, 506–512. (c) Dubois, L. H.; Nuzzo, R. G. *Annu. Rev. Phys. Chem.* **1992**, *43*, 437–463.
- (5) (a) Walczak, M. M.; Chung, C.; Stole, S. M.; Widrig, C. A.; Porter, M. D. *J. Am. Chem. Soc.* **1991**, *113*, 2370–2378. (b) Fenter, P.; Eisenberger, P.; Li, J.; Camillone, N., III; Bernasek, S.; Scoles, G.; Ramanarayanan, T. A.; Liang, K. S. *Langmuir* **1991**, *7*, 2013–2016. (c) Laibinis, P. E.; Fox, M. A.; Folkers, J. P.; Whitesides, G. M. *Langmuir* **1991**, *7*, 3167–3173. (d) Laibinis, P. E.; Whitesides, G. M.; Allara, D. L.; Tao, Y.-T.; Parikh, A. N.; Nuzzo, R. G. *J. Am. Chem. Soc.* **1991**, *113*, 7152–7167. (e) Sellers, H.; Ulman, A.; Shnidman, Y.; Eilers, J. E. *J. Am. Chem. Soc.* **1993**, *115*, 9389–9401.
- (6) Tarlov, M. J. *Langmuir* **1992**, *8*, 80–89.

- (7) (a) Strong, L.; Whitesides, G. M. *Langmuir* **1988**, *4*, 546–558. (b) Nuzzo, R. G.; Dubois, L. H.; Allara, D. L. *J. Am. Chem. Soc.* **1990**, *112*, 558–569. (c) Porter, M. D.; Bright, T. M.; Allara, D. L.; Chidsey, C. E. D. *J. Am. Chem. Soc.* **1987**, *109*, 3559–3568. (d) Bain, C. D.; Troughton, E. B.; Tao, Y.-T.; Evall, J.; Whitesides, G. M.; Nuzzo, R. G. *J. Am. Chem. Soc.* **1989**, *111*, 321–335.

Chart 2. Hexagonal Ag Lattice



Shaded circles and open circles refer to alkyl groups projecting above and below the Ag-S plane.

the strength of the Ag-S interaction and has previously been observed on single-crystal Ag surfaces treated with H₂S, SO₂, S₂, and even CH₃SSCH₃.¹¹ While structural differences between this 2-D film and the 3-D AgSR solid are obvious, a number of features bear strong similarity. In particular, both materials have hexagonal lattices of Ag and S, thiolate anion-Ag⁺ interactions, triply bridging S, and perpendicular or nearly-perpendicular alkyl chains.

Despite their relevance to materials chemistry, the structures of these AgSR solids are poorly understood. For example, the color of these compounds varies from white to almost white to yellow, depending on synthetic conditions.^{1,3,12} Moreover, for $n = 3-17$, the white compounds turn yellow upon melting. A second unresolved issue concerns the alkyl chain orientation.

- (8) (a) Camillone, N., III; Chidsey, C. E. D.; Eisenberger, P.; Fenter, P.; Li, J.; Liang, K. S.; Liu, G.-Y.; Scoles, G. *J. Chem. Phys.* **1993**, *99*, 744-747. (b) Fenter, P.; Eberhardt, A.; Eisenberger, P. *Science* **1994**, *266*, 1216-1218. (c) Fenter, P.; Eisenberger, P.; Liang, K. S. *Phys. Rev. Lett.* **1993**, *70*, 2447-2450. (d) Stranick, S. J.; Kamna, M. M.; Krom, K. R.; Parikh, A. N.; Allara, D. L.; Weiss, P. S. *J. Vac. Sci. Technol., B* **1994**, *12*, 2004-2007. (e) Nuzzo, R. G.; Korenic, E. M.; Dubois, L. H. *J. Chem. Phys.* **1990**, *93*, 767-773.
- (9) (a) Finklea, H. O.; Ravenscroft, M. S.; Snider, D. A. *Langmuir* **1993**, *9*, 223-227. (b) Finklea, H. O.; Snider, D. A.; Fedyk, J.; Sabatani, E.; Gafni, Y.; Rubinstein, I. *Langmuir* **1993**, *9*, 3660-3667. (c) Chidsey, C. E. D.; Loiacono, D. N. *Langmuir* **1990**, *6*, 682-691. (d) Groat, K. A.; Creager, S. E. *Langmuir* **1993**, *9*, 3668-3675. (e) Creager, S. E.; Collard, D. M.; Fox, M. A. *Langmuir* **1990**, *6*, 1617-1620. (f) Chidsey, C. E. D. *Science* **1991**, *251*, 919-922. (g) Guo, L.-H.; Facci, J. S.; McLendon, G. *J. Phys. Chem.* **1995**, *99*, 4106-4112. (h) Guo, L.-H.; Facci, J. S.; McLendon, G. *J. Phys. Chem.* **1995**, *99*, 8458-8461. (i) Hockett, L. A.; Creager, S. E. *Langmuir* **1995**, *11*, 2318-2321. (j) Ravenscroft, M. S.; Finklea, H. O. *J. Phys. Chem.* **1994**, *98*, 3843-3850. (k) Rowe, G. K.; Carter, M. T.; Richardson, J. N.; Murray, R. W. *Langmuir* **1995**, *11*, 1797-1806. (l) Smalley, J. F.; Feldberg, S. W.; Chidsey, C. E. D.; Linford, M. R.; Newton, M. D.; Liu, Y.-P. *J. Phys. Chem.* **1995**, *99*, 13141-13149.
- (10) (a) Herr, B. R.; Mirkin, C. A. *J. Am. Chem. Soc.* **1994**, *116*, 1157-1158. (b) Everett, W. R.; Welch, T. L.; Reed, L.; Fritsch-Faules, I. *Anal. Chem.* **1995**, *67*, 292-298. (c) Carter, M. T.; Rowe, G. K.; Richardson, J. N.; Tender, L. M.; Terrill, R. H.; Murray, R. W. *J. Am. Chem. Soc.* **1995**, *117*, 2896-2899. (d) Cruaños, M. T.; Drickamer, H. G.; Faulkner, L. R. *Langmuir* **1995**, *11*, 4089-4097. (e) Gardner, T. J.; Frisbie, C. D.; Wrighton, M. S. *J. Am. Chem. Soc.* **1995**, *117*, 6927-6933. (f) Gorman, C. B.; Biebuyck, H. A.; Whitesides, G. M. *Chem. Mater.* **1995**, *7*, 526-529. (g) Terrill, R. H.; Postlethwaite, T. A.; Chen, C.-H.; Poon, C.-D.; Terzis, A.; Chen, A.; Hutchison, J. E.; Clark, M. R.; Wignall, G.; Londono, J. D.; Superfine, R.; Falvo, M.; Johnson, C. S., Jr.; Samulski, E. T.; Murray, R. W. *J. Am. Chem. Soc.* **1995**, *117*, 12537-12548. (h) Han, T.; Beebe, T. P., Jr. *Langmuir* **1994**, *10*, 2705-2709. (i) McDermott, C. A.; McDermott, M. T.; Green, J.-B.; Porter, M. D. *J. Phys. Chem.* **1995**, *99*, 13257-13267. (j) Takami, T.; Delamarche, E.; Michel, B.; Gerber, Ch.; Wolf, H.; Ringsdorf, H. *Langmuir* **1995**, *11*, 3876-3881.
- (11) (a) Rovida, G.; Pratesi, F. *Surf. Sci.* **1981**, *104*, 609-624. (b) Schwaha, K.; Spencer, N. D.; Lambert, R. M. *Surf. Sci.* **1979**, *81*, 273-284. (c) Harris, A. L.; Rothberg, L.; Dubois, L. H.; Levinos, N. J.; Dhar, L. *Phys. Rev. Lett.* **1990**, *64*, 2086-2089.
- (12) Chadha, R. K.; Kumar, R.; Tuck, D. G. *Can. J. Chem.* **1987**, *65*, 1336-1342.

The only evidence for the perpendicular orientation depicted in Chart 1, as opposed to a tilted alkyl geometry, is based on the supposition of a fully extended, all-trans chain and a calculated Ag-S slab thickness of 1.0-1.5 Å,¹ but no spectroscopic evidence exists for either assumption.

We describe herein Raman,¹⁰⁹Ag cross polarization magic angle spinning (CPMAS) NMR,^{13a,14} X-ray diffraction (XRD),^{13C} CPMAS NMR, and absorbance measurements on three forms of solid AgS(CH₂)₃CH₃, a white all-trans compound (**T**), a bright yellow conformational isomer with a gauche geometry about the C(1)-C(2) bond (**G**), and a pale yellow phase containing both trans and gauche phases (**G/T**). Conditions leading to formation of **G**, **T**, and **G/T** have been elucidated; the color change associated with the **T** → **G** transformation results from changes in the Ag⁺ coordination environment and is inconsistent with a decrease in coordination number. **T** is less stable than **G**, converting cleanly with an activation energy (E_a) of roughly 60 kJ/mol. XRD experiments indicate an interlayer spacing increase from 15.56 Å in **T** to 16.88 Å in **G**. Moreover, geometric constraints imposed by ¹⁰⁹Ag NMR data coupled with bond lengths from X-ray crystallographically-characterized Ag thiolate model compounds¹⁵ lead to three additional conclusions about the structure of these materials: (i) There exist two different three-coordinate environments for Ag⁺ in both **T** and **G**. (ii) The identification of solely three-coordinate Ag⁺ in **G** shows that the μ₃-bridging → μ₂-bridging transformation in all-trans AgSR compounds proposed to occur upon melting is inconsistent with the associated appearance of gauche environments and the concurrent color change from white to yellow. (iii) The S-S spacing in these materials is between 4.4-4.8 Å, values that correspond well to those previously observed for organothiols SAMs on well-defined Ag surfaces.⁵

Experimental Section

Materials. AgNO₃ (99+%, Aldrich) and CH₃(CH₂)₃SH (99%, Aldrich), spectroscopic grade CH₃CN and CH₃OH (Fisher Scientific), and C₆H₆ (J. T. Baker, Baker Analyzed reagent) were used as received. Water was distilled and deionized on a Barnstead Nanopure Analytical Water Filtration System (18 MΩ). Syntheses were carried out in Al-foil-wrapped flasks to protect reactants and products from light exposure. Elemental analyses were performed by Schwarzkopf Microanalytical Laboratory.

Synthesis of AgS(CH₂)₃CH₃ (Form T). A 1.67 g sample of AgNO₃ in 20 mL of H₂O was added dropwise with stirring to 0.90 g of butanethiol in 20 mL of CH₃CN. The pale yellow precipitate was filtered off, and 1.4 g of wet product was placed in an Erlenmeyer flask. A 20 mL portion of CH₃OH and 100 mL of C₆H₆ were added slowly with heating to the precipitate, and the resulting suspension was refluxed for 25 min and hot-filtered. The filtrate was dried in air, yielding a white solid, mp 140-142 °C. Anal. Calcd for C₄H₉AgS:

- (13) (a) Fijolek, H. G.; Oriskovich, T. O.; Benesi, A. J.; González-Duarte, P.; Natan, M. J. *Inorg. Chem.* **1996**, *35*, 797-799. (b) Narula, S. S.; Mehra, R. K.; Winge, D. R.; Armitage, I. M. *J. Am. Chem. Soc.* **1991**, *113*, 9354-9358. (c) Narula, S. S.; Winge, D. R.; Armitage, I. M. *Biochemistry* **1993**, *32*, 6773-6787.
- (14) Merwin, L. H.; Sebald, A. *J. Magn. Reson.* **1992**, *97*, 628-631.
- (15) (a) Block, E.; Gernon, M.; Kang, H.; Ofori-Okai, G.; Zubieta, J. *Inorg. Chem.* **1989**, *28*, 1263-1271. (b) Block, E.; Macherone, D.; Shaikh, S. N.; Zubieta, J. *Polyhedron* **1990**, *9*, 1429-1432. (c) Dance, I. G. *Inorg. Chim. Acta* **1977**, *25*, L17-L18. (d) Dance, I. G. *Aust. J. Chem.* **1978**, *31*, 2195-2206. (e) Dance, I. G. *Inorg. Chem.* **1981**, *20*, 1487-1492. (f) Dance, I. G.; Fitzpatrick, L. J.; Rae, A. D.; Scudder, M. L. *Inorg. Chem.* **1983**, *22*, 3785-3788. (g) Dance, I. G. *Polyhedron* **1988**, *7*, 2205-2207. (h) González-Duarte, P.; Sola, J.; Vives, J.; Solans, X. *J. Chem. Soc., Chem. Commun.* **1987**, 1641-1642. (i) Henkel, G.; Betz, P.; Krebs, B. *Angew. Chem., Int. Ed. Engl.* **1987**, *26*, 145-146. (j) Henkel, G.; Krebs, B.; Betz, P.; Fietz, H.; Saatkamp, K. *Angew. Chem., Int. Ed. Engl.* **1988**, *27*, 1326-1329. (k) Hong, S.-H.; Olin, A.; Hesse, R. *Acta Chem. Scand., Ser. A* **1975**, *29*, 583-589. (l) Tang, K.; Aslam, M.; Block, E.; Nicholson, T.; Zubieta, J. *Inorg. Chem.* **1987**, *26*, 1488-1497. (m) Tang, K.; Yang, J.; Yang, Q.; Tang, Y. *J. Chem. Soc., Dalton Trans.* **1989**, 2297-2302.

C, 24.38; H, 4.60; S, 16.27; Ag, 54.74. Found: C, 24.38; H, 4.57; S, 16.24; Ag, 54.49.

Synthesis of $\text{AgS}(\text{CH}_2)_3\text{CH}_3$ (Form G/T). A 3.79 g amount of AgNO_3 in 60 mL of H_2O was added dropwise with stirring to 2.02 g of butanethiol in 60 mL of CH_3CN . The very pale yellow precipitate was filtered off, washed with H_2O , and allowed to dry in air. The compound slowly turned yellow on drying. Part of the solid melted at 140–142 °C; the remaining solid decomposed at 185 °C. Anal. Found: C, 24.27; H, 4.69; S, 15.99; Ag, 55.01.

Synthesis of $\text{AgS}(\text{CH}_2)_3\text{CH}_3$ (Form G). A 1.67 g sample of AgNO_3 in 60 mL of CH_3CN was added dropwise with stirring to 0.90 g of butanethiol in 20 mL of CH_3CN . The resulting white precipitate turned bright yellow after approximately 10 min at room temperature, and the mixture was stirred for an additional 45 min. The precipitate was filtered off, washed with CH_3CN , and dried in air; mp 185 °C dec. Anal. Found: C, 21.44; H, 4.10; S, 14.29; Ag, 54.29; N, 0.99.

Temperature Dependence of the T → G Conversion. The same synthetic procedure as used for preparation of **G** was employed, with the modification that the entire bolus of AgNO_3 was added at once with stirring, at temperatures ranging from 267 to 296 K. The time for the solution to develop the first visibly discernible yellow color was recorded.

Instrumentation. Diffuse reflectance electronic spectra were obtained with a Perkin-Elmer Lambda 9 double-beam, double-monochromator UV–visible/infrared spectrophotometer using an integrating sphere with BaSO_4 as the reference. Raman spectra were obtained using the 647.1 nm line of a Spectra Physics Model 164 laser equipped with an Excitek mixed-gas (Ar^+/Kr^+) plasma tube. Detection was carried out using a Spex 1877 triple monochromator equipped with a 1200 groove/mm spectrograph grating, a 600 groove/mm filter stage grating, and a UV-coated, liquid- N_2 -cooled CCD detector. A more detailed description of this apparatus is found elsewhere.¹⁶ Solid state ^{109}Ag and ^{13}C spectra were acquired at 294 K on a Chemagnetics CMX-300 spectrometer operating in the quadrature mode at 13.85 MHz for ^{109}Ag , 74.78 MHz for ^{13}C , and 297.37 MHz for ^1H . A Doty Scientific multinuclear double-tuned 10 mm Supersonic probe was used for ^{109}Ag experiments, and a Chemagnetics multinuclear double-tuned 7.5 mm Pencil probe was used for ^{13}C experiments. AgOCCH_3 was used as a secondary standard reference [382.7, 401.2 ppm relative to AgNO_3]^{13a} for ^{109}Ag NMR experiments, and hexamethylbenzene [132.21 ppm relative to $\text{Si}(\text{CH}_3)_4$] was used as the reference for ^{13}C NMR experiments. X-ray diffraction data were obtained in steps of $0.02^\circ 2\theta$ with a Rigaku Geigerflex automated diffractometer using graphite-monochromated $\text{Cu K}\alpha$ radiation and Si as an external standard.

Results

Syntheses of T, G/T, and G. Dance et al. have previously synthesized a series of layered Ag alkanethiolate compounds:¹ compound **T** in this work is identical in appearance and physical characteristics to the white all-trans $\text{AgS}(\text{CH}_2)_3\text{CH}_3$ compound synthesized under other experimental conditions.^{1,3,11} Initial attempts to synthesize white all-trans $\text{AgS}(\text{CH}_2)_3\text{CH}_3$ under conditions other than those previously published led to syntheses in $\text{CH}_3\text{CN}/\text{H}_2\text{O}$, which produced a pale yellow compound subsequently determined by XRD to be a mixture of layered all-trans $\text{AgS}(\text{CH}_2)_3\text{CH}_3$ and an unknown layered phase. Confirmation of the mixed-phase character of this pale yellow compound is seen in its melting point behavior, in which part of the solid melts at the same temperature as the all-trans compound (140–142 °C) and part decomposes at 185 °C. Both the all-trans (**T**) and the mixed-phase (**G/T**) compounds give satisfactory elemental analyses.

Further attempts to isolate the unknown phase led to the observation that, under ambient conditions in CH_3CN , the white $\text{AgS}(\text{CH}_2)_3\text{CH}_3$ compound turned rapidly and irreversibly to bright yellow; the XRD and melting point of the bright yellow compound (form **G**) indicated that it was the unknown phase

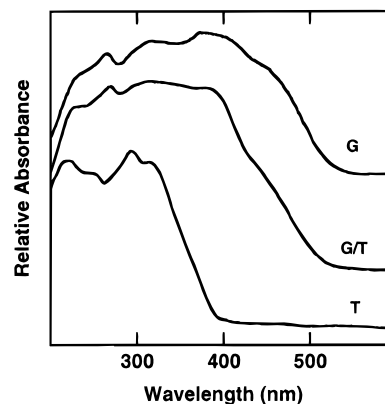


Figure 1. Solid-state diffuse reflectance spectra of $\text{AgS}(\text{CH}_2)_3\text{CH}_3$ compounds **G** (top), **G/T** (middle), and **T** (bottom). For clarity, spectra are offset vertically.

previously seen in the pale yellow mixture. Synthesis of the all-trans form **T** was initially carried out under a N_2 atmosphere, and isolation involved the use of a vacuum. When the vacuum was released, we observed the **T** → **G** transformation, leading us to suspect the involvement of O_2 . In fact, sample warming was responsible: synthesis of **T** at room temperature under a rigorously inert atmosphere leads to **G**.

Sensitivity in AgSR chemistry to synthetic conditions has been briefly described^{1,3} but never quantified. Further investigation revealed that the rate of conversion from **T** to **G** is extremely dependent on reaction conditions, with decreased conversion rates at lower reactant concentration, in more basic solutions, at higher HSR: AgNO_3 ratios, decreased mass transport (i.e. slower stirring or addition rate), and lower temperatures. A very rough estimate of activation energy can be obtained from a plot of $\ln(k)$ vs temperature⁻¹, where k^{-1} is the time required for appearance of yellow color as judged by eye. Such a plot is linear (Supporting Information) and yields an activation energy (E_a) of ≈ 60 kJ/mol.

Previous work on structurally characterized Ag thiolates led to the conclusion that trigonally-coordinated Ag thiolates are yellow, while solely two-coordinate species are white.¹⁵ The pale yellow color of **G/T** and intense yellow color of **G** arise from low-energy ligand-to-metal charge transfer bands; a similar trend toward lower energy transitions upon increasing coordination of d^{10} metal complexes was previously observed.¹⁷ In the solid state reflectance spectra (Figure 1), **T** has peaks or shoulders at 220, 251, 293, and 315 nm, **G/T** at 228, 266, 298, 380, and 440 nm, and **G** at 230, 265, 315, 380, and 449 nm.

The intense color of **G** is unusual in Ag thiolate chemistry.¹⁵ Unfortunately, the extreme insolubility of neutral AgSR compounds with primary alkyl groups precludes measurement of solution state optical spectra for **T**, **G/T**, and **G** once isolated. Optical measurements have been carried out on soluble Ag^+ -substituted metalloproteins—with Ag^+ coordination environments consisting solely of (primary) $-\text{SCH}_2$ side chains from cysteine^{18,19}—either via absorbance²⁰ or through acquisition of a fluorescence excitation spectrum.²¹ In both cases, neither peaks nor shoulders were observed at wavelengths longer than 300 nm. However, a soluble species formed by reaction of Ag^+ and $\text{HSCH}_2\text{CH}_2\text{OH}$ in Tris buffer at pH 8.0 has an intense

(16) Grabar, K. C.; Allison, K. J.; Baker, B. E.; Bright, R. M.; Brown, K. R.; Freeman, R. G.; Fox, A. P.; Keating, C. D.; Musick, M. D.; Natan, M. J. *Langmuir* **1996**, *12*, 2353–2361.

(17) Kägi, J. H. R.; Schäffer, A. *Biochemistry* **1988**, *27*, 8509–8515.
 (18) Fürst, P.; Hu, S.; Hackett, R.; Hamer, D. *Cell* **1988**, *55*, 705–717.
 (19) *Metallothioneins*; Stillman, M. J., Shaw, C. F., III, Suzuki, K. T., Eds.; VCH Publishers: New York, 1991.
 (20) Zelazowski, A. J.; Gasyana, Z.; Stillman, M. J. *J. Biol. Chem.* **1989**, *264*, 17091–17099.
 (21) Casas-Finet, J. R.; Hu, S.; Hamer, D.; Karpel, R. L. *Biochemistry* **1992**, *31*, 6617–6626.

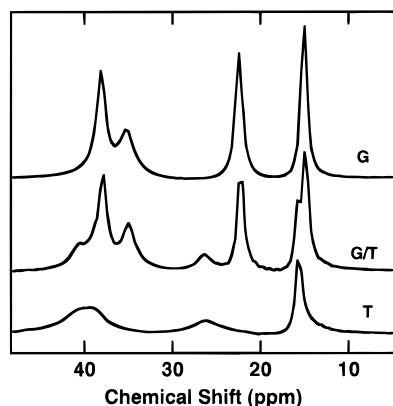


Figure 2. ^{13}C CPMAS NMR spectra of **G** (top), **G/T** (middle), and **T** (bottom) forms of $\text{AgS}(\text{CH}_2)_3\text{CH}_3$. Conditions: pulse delay, 4 s; contact time, 5 ms; ring-down delay, 20 μs ; spinning rate, 3 kHz. Transients: **G**, 864; **G/T**, 1104; **T**, 1896.

absorbance peak centered around 365 nm;²² we have noted similar optical properties in solutions of AgSR with secondary and tertiary alkyl groups, and these features are retained in the solid state.²³

It is important to note that features in the optical spectrum of **G/T** appear to be a near superposition of those seen in the spectra for **G** and **T**. Moreover, this is true for all the spectral properties described below (^{13}C , ^{109}Ag , Raman, XRD). Accordingly, the imperfect elemental analysis for **G**, which appears to result from the inclusion of $\approx 1\%$ N (but not from CH_3CN , since the C:S ratio is correct), in no way impacts the results reported herein. It is worth noting that the slight deviation in Ag percentage in **G** is identical to that reported by Chadha et al. for $\text{AgS}(\text{CH}_2)_3\text{CH}_3$ obtained by anodic dissolution of Ag metal in a solution containing only $\text{CH}_3(\text{CH}_2)_3\text{SH}$ and CH_3CN .¹²

Molecular Structures of T, G/T, and G. The possibility that the color differences in **T**, **G/T**, and **G** result from changes in metal coordination environment suggested the use of probes more sensitive than electronic spectroscopy. An obvious choice is NMR, and Figure 2 depicts the ^{13}C CPMAS NMR spectra of compounds **G**, **T**, and **G/T**. Four peaks due to the carbon backbone are visible in the spectrum of compound **T** at 15.8, 26.4, 39.3, and 40.5 ppm. These same four peaks are visible in the spectrum of compound **G/T**, in some cases as shoulders of new peaks. Four new peaks shifted upfield are seen for **G** (and also for **G/T**) at 15.0, 22.1, 35.0, and 37.8 ppm. The locations for the ^{13}C chemical shifts of these compounds are in the regions expected for alkanes.²⁴ More importantly, the systematic 1–5 ppm upfield shift for each peak in the spectrum of **G** indicated the presence of a gauche bond in the C backbone, a conclusion based on numerous ^{13}C NMR studies of alkane conformations.²⁵

Raman studies showed that this gauche interaction was present at C(1)–C(2). Low-wavenumber Raman spectra of the three $\text{AgS}(\text{CH}_2)_3\text{CH}_3$ compounds are shown in Figure 3. A tremendous amount of data exists on Raman spectra of organothiols in solution²⁶ and arganothiols adsorbed to Ag surfaces. For the latter, detailed surface-enhanced Raman

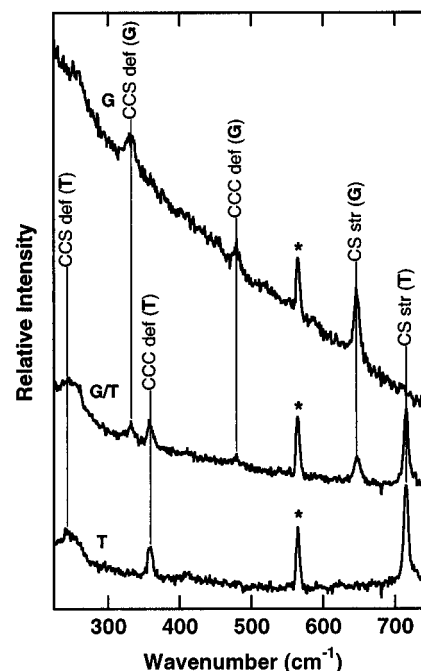


Figure 3. Raman spectra of **G** (top), **G/T** (middle), and **T** (bottom) forms of $\text{AgS}(\text{CH}_2)_3\text{CH}_3$. Conditions: 647.1-nm laser line, 20 mW at sample, 10-s integration time. The symbol * refers to a laser plasma line. Bands assigned to gauche (**G**) and trans (**T**) conformations of the carbon backbone are so marked.

scattering (SERS)²⁷ studies exist for both for aromatic²⁸ and aliphatic thiols,^{29,30} including butanethiol.³¹ This body of work allows definitive assignment of several bands to gauche and trans conformers of the butanethiolate ligand. **T** has bands at 243, 359, 410, and 715 cm^{-1} , while **G** exhibits Raman peaks at 253, 330, 479, and 646 cm^{-1} . Information regarding the conformation of the C–C bond adjacent to the S is contained in two $\nu(\text{C}–\text{S})$ bands at 656 and 730 cm^{-1} for neat butanethiol, which have been assigned to gauche and trans C(1)–C(2) vibrations, respectively.^{26,28–31} When butanethiol binds to Ag, these bands shift to lower frequency and are seen at 646 cm^{-1}

(22) Andersson, L.-O. *J. Polymer Sci., Part A* **1972**, *10*, 1963–1973.

(23) Fijolek, H. G.; Natan, M. J. Manuscript in preparation.

(24) Lindeman, L. P.; Adams, J. Q. *Anal. Chem.* **1971**, *43*, 1245–1252.

(25) (a) Ishikawa, S.; Kuroso, H.; Ando, I. *J. Mol. Struct.* **1991**, *248*, 361–372. (b) Okazaki, M.; McDowell, C. A. *J. Mol. Struct.* **1984**, *118*, 149–156. (c) Ando, I.; Yamanobe, T.; Sorita, T.; Komoto, T.; Sato, H.; Deguchi, K.; Imanari, M. *Macromolecules* **1984**, *17*, 1955–1958.

(26) Dollish, F. R.; Fateley, W. G.; Bentley, F. F. *Characteristic Raman Frequencies of Organic Compounds*; John Wiley and Sons: New York, 1974; Chapter 5 and references therein.

(27) (a) Brandt, E. S.; Cotton, T. M. In *Investigations of Surfaces and Interfaces, Part B*; Rossiter, B. W., Baetzold, R. C., Eds; John Wiley and Sons: New York, 1993; pp 633–718. (b) Birke, R. L.; Lu, T.; Lombardi, J. R. in *Techniques for Characterization of Electrodes and Electrochemical Processes*; Varma, R. and Selman, J. R., Eds; John Wiley and Sons: New York, 1991; pp 211–277.

(28) (a) Sandroff, C. J.; Herschbach, D. R. *J. Phys. Chem.* **1982**, *86*, 3277–3279. (b) Xue, G.; Ma, M.; Zhang, J.; Lu, Y. *J. Colloid Interface Sci.* **1992**, *150*, 1–6. (c) Osawa, M.; Matsuda, N.; Yoshii, K.; Uchida, I. *J. Phys. Chem.* **1994**, *98*, 12702–12707. (d) Lee, T. G.; Kim, K.; Kim, M. S. *J. Phys. Chem.* **1991**, *95*, 9950–9955. (e) Lee, T. G.; Kim, K.; Kim, M. S. *J. Raman Spectrosc.* **1991**, *22*, 339–344. (f) Lee, T. G.; Yeom, H. W.; Oh, S.-J.; Kim, K.; Kim, M. S. *Chem. Phys. Lett.* **1989**, *163*, 98–105. (g) Cho, S. H.; Han, H. S.; Jang, D.-J.; Kim, K.; Kim, M. S. *J. Phys. Chem.* **1995**, *99*, 10594–10599. (h) Joo, T. H.; Kim, M. S.; Kim, K. *J. Raman Spectrosc.* **1987**, *18*, 57–60.

(29) (a) Joo, T. H.; Kim, K.; Kim, M. S. *J. Phys. Chem.* **1986**, *90*, 5816–5819. (b) Joo, T. H.; Kim, M. S.; Kim, K. *J. Mol. Struct.* **1987**, *160*, 81–89. (c) Watanabe, T.; Maeda, H. *J. Phys. Chem.* **1989**, *93*, 3258–3260. (d) Kwon, C. K.; Kim, M. S.; Kim, K. *J. Mol. Struct.* **1987**, *162*, 201–210. (e) Kwon, C. K.; Kim, M. S.; Kim, K. *J. Raman Spectrosc.* **1989**, *20*, 575–580. (f) Lee, S. B.; Kim, K.; Kim, M. S.; Oh, W. S.; Lee, Y. S. *J. Mol. Struct.* **1993**, *296*, 5–13.

(30) Sandroff, C. J.; Garoff, S.; Leung, K. P. *Chem. Phys. Lett.* **1983**, *96*, 547–551.

(31) (a) Bryant, M. A.; Pemberton, J. E. *J. Am. Chem. Soc.* **1991**, *113*, 3629–3637. (b) Bryant, M. A.; Pemberton, J. E. *J. Am. Chem. Soc.* **1991**, *113*, 8284–8293. (c) Joo, T. H.; Kim, K.; Kim, M. S. *J. Mol. Struct.* **1987**, *158*, 265–274. (d) Nandy, S. K.; Mukherjee, D. K. *Indian J. Phys.* **1974**, *48*, 81–86. (e) Sobocinski, R. L.; Bryant, M. A.; Pemberton, J. E. *J. Am. Chem. Soc.* **1990**, *112*, 6177–6183. (f) Pemberton, J. E.; Bryant, M. A.; Sobocinski, R. L.; Joa, S. L. *J. Phys. Chem.* **1992**, *96*, 3776–3782.

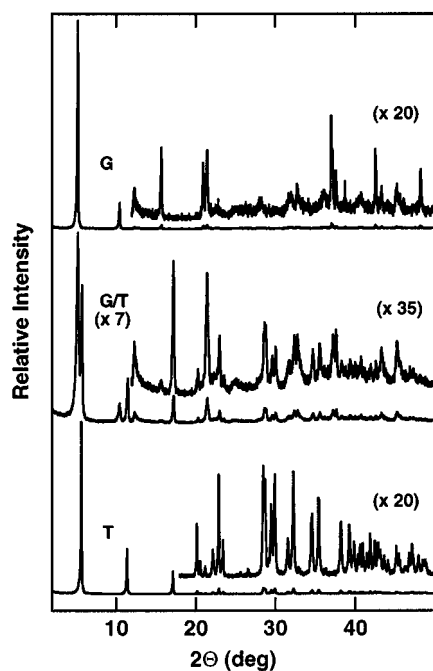


Figure 4. X-ray powder diffraction patterns of **G** (top), **G/T** (middle), and **T** (bottom) forms of $\text{AgS}(\text{CH}_2)_3\text{CH}_3$. Above each diffraction pattern are magnified views of large 2θ regions.

for compound **T** and 715 cm^{-1} for **G**. This result shows that the white compound **T** exhibits an all-trans geometry. In contrast, the butanethiolate in the bright yellow compound **G** exists in the gauche C(1)–C(2) conformation, evidenced by the complete absence of the trans C–S stretch. Several other bands between 250 and 600 cm^{-1} (Figure 3) are in agreement with this assignment. Compound **G/T** once again exhibits a mixture of the bands seen for the two compounds separately. Identification of yellow **G** as the C(1)–C(2) gauche isomer and **T** as the all-trans form comprises the first molecular information regarding the origin of color in these compounds.

To see whether the **T** to **G** conversion influenced the layer structure, X-ray diffraction (XRD) studies were carried out on the three $\text{AgS}(\text{CH}_2)_3\text{CH}_3$ compounds (Figure 4). XRD studies of layered silver salts dates back >40 years, when the technique was used to identify long-chain fatty acids.³² Examination of the data indicates that two different phases appear to be present in compound **G/T**, one of which is shared with compound **T** and one of which is present in **G**. Dance et al. previously postulated a monoclinic unit cell with $a \approx 8.7\text{ \AA}$, interlayer spacing $b = 15.45\text{ \AA}$, $c \approx 4.35\text{ \AA}$, and $\beta \approx 120^\circ$ for their $\text{AgS}(\text{CH}_2)_3\text{CH}_3$ compound,¹ which compound **T** very closely resembles.

From the d spacing data for compounds in these studies, interlayer spacings (b) for the pronounced $(0k0)$ reflections were calculated using $b = kd$, where k is the order of the reflection. The data show that the interlayer spacings present in **T** (15.56 \AA) and **G** (16.88 \AA) are essentially identical to those seen in compound **G/T** (15.45 and 16.90 \AA). This supports the melting point evidence that two distinct phases exist in **G/T**. Additional reflections present in **G** which are not seen in **T** or assigned to $0k0$ reflections confirm that there are structural differences between these two compounds other than the interlayer spacing. Dance et al. previously noted the presence of numerous $\{h0l\}$ spacings for a series of layered AgSR compounds;¹ their presence is indicative of registry between layers, and they in fact were used to approximate the monoclinic unit cell. Our

attempts to solve the unit cell structure without any approximations or constraints used by Dance were unsuccessful. The lack of exact agreement between the expected and observed reflections indicate a symmetry lowering, a finding we confirm below. The important point is that while the in-plane structure of these compounds is uncertain, the interlayer spacing is not: the large number of lines in the X-ray diffraction spectra indicate a high degree of order for **T**, **G/T**, and **G**.

Further verification of the existence of the gauche conformation of the alkane chain in **G**, as well as proof of distortion from a purely hexagonal lattice (Chart 2), comes from ^{109}Ag CPMAS NMR, a technique that is extremely sensitive to the coordination environment of Ag^+ and provides a detailed view of Ag–S bonding (Figure 5). We observed a dramatic improvement in signal/noise for **G** relative to **T**. Since the efficiency of spin transfer from ^1H to ^{109}Ag in this experiment increases with decreasing Ag–H distance,^{13a} the NMR data indicate close proximity of a hydrogen to the Ag^+ plane. Chart 3 shows that if the alkyl chain is perpendicular to the Ag^+ plane, the trans–gauche interconversion places a C(3) H atom very close to the Ag^+ plane. Note, however, that trans–gauche isomerizations in *tilted* alkane chains also increase the proximity of the C(3) H to the surface (Supporting Information).

Table 1 lists the isotropic chemical shifts, chemical shift anisotropies ($\Delta\sigma$), and asymmetry factors (η) for the two unique Ag^+ environments present in each compound. Comparison with analogous ^{109}Ag NMR data for structurally-characterized Ag thiolates^{13a} and for the protein Ag–S clusters of Ag₈-(metallothionein) in solution^{13b,c} permits the following conclusions to be drawn about the Ag coordination environments in $\text{AgS}(\text{CH}_2)_3\text{CH}_3$: (i) The isotropic chemical shifts for both Ag^+ environments in the gauche isomer appear in the strictly three-coordinate range, while those for **3** and **4** lie between two-coordinate and three-coordinate regimes. (ii) The high $\Delta\sigma$ values for **1**, **3**, and **4** indicate highly distorted environments. (iii) The low $\Delta\sigma$ and the presence of a symmetry axis ($\eta = 0$) in **2** is consistent with a trigonal planar geometry. (iv) Environment **3** also exhibits axial symmetry; coupled with the high $\Delta\sigma$ and upfield chemical shift, a Y-shaped geometry with two short Ag–S bonds and one long (secondary) Ag–S bond is proposed. Chart 3 shows the predicted geometries for the $\eta = 0$ Ag^+ sites in the gauche and all-trans $\text{AgS}(\text{CH}_2)_3\text{CH}_3$, incorporating average lengths for three-coordinate (2.55 \AA) and secondary (3.0 \AA) Ag–S bonds.^{1,13a,15}

Preliminary studies on longer chain $\text{AgS}(\text{CH}_2)_n\text{CH}_3$ compounds ($n = 5, 7, 9, 11$) also indicate plasticity in Ag^+ coordination environment and alkyl chain conformation. When prepared at room temperature, each of these compounds was white, but when synthesized in hot CH_3CN , they turned yellow and subsequently decomposed. More importantly, for both $n = 7$ and 11 , temperature-dependent Raman spectra indicated changes in Ag–S modes and in C-backbone conformation-sensitive bands occurred at temperatures as low as $100\text{ }^\circ\text{C}$ below the melting points of the compounds²³ (where color changes from white to intense yellow occur).³

Discussion

Layered $\text{AgS}(\text{CH}_2)_3\text{CH}_3$ exists in two distinct phases, a fully extended, all-trans form (**T**) that is white and a form exhibiting a gauche conformation (**G**) at C(1)–C(2) that is bright yellow. The latter is more stable, as evidenced by the temperature-dependent conversion of **T** to **G** and by the substantially higher melting point. No external reagents are required to effect this transformation. Information gleaned from ^{109}Ag NMR spectra indicate the presence of two distinct Ag^+ environments in both **T** and **G**; for the latter both are strictly three-coordinate, while

(32) Matthews, F. W.; Warren, G. G.; Mitchell, J. H. *Anal. Chem.* **1950**, *22*, 514–519.

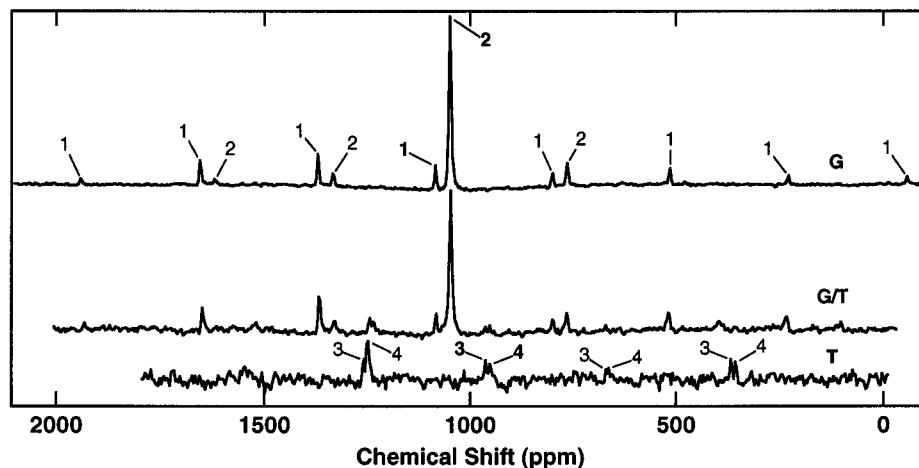


Figure 5. ^{109}Ag CPMAS NMR spectra of $\text{AgS}(\text{CH}_2)_3\text{CH}_3$ forms **G** (top), **G/T** (middle), and **T** (bottom). Conditions: pulse delay, 3 s; contact time, 15 ms; ring-down delay, 40 μs . Top: spinning rate, 3.9 kHz; 5152 transients. Bottom: spinning rate, 4.1 kHz; 29024 transients. See Table 1 for peak assignments; bold labels correspond to isotropic peaks.

Chart 3. Chain Orientations and Coordination Environments for $\text{AgS}(\text{CH}_2)_3\text{CH}_3$

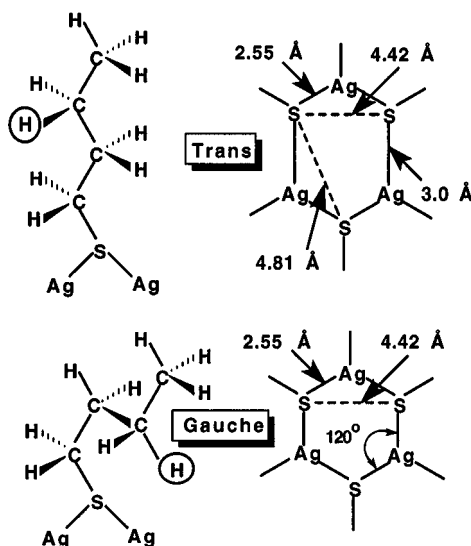


Table 1. Chemical Shift Parameters for $\text{AgS}(\text{CH}_2)_3\text{CH}_3$ Compounds

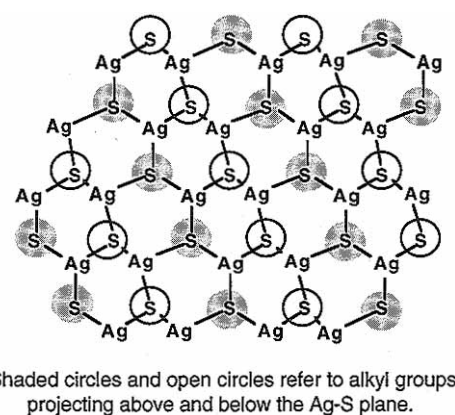
$\text{AgS}(\text{CH}_2)_3\text{CH}_3$ conformn	type of Ag environment	isotropic chem shift (ppm)	chem shift anisotropy ($\Delta\sigma$, ppm) ^a	asymmetry factor (η) ^a
all-gauche	1	1083	-1863	0.56
	2	1048	512	0.00
all-trans	3	962	-1703	0.00
	4	952	-1631	0.61

^a For definitions of $\Delta\sigma$ and η , see ref 13 and: Fyfe, C. A. *Solid State NMR for Chemists*; CRC Press: Guelph, Ontario, Canada, 1983.

the former exhibits chemical shifts between those previously observed for two- and three-coordinate Ag thiolates.¹³

Taken together, what do these spectroscopic data reveal about the structure of layered $\text{AgS}(\text{CH}_2)_3\text{CH}_3$? The presence of two distinct Ag^+ environments in both **T** and **G** indicates that the regular hexagonal lattice illustrated in Chart 1 is an oversimplification: all Ag^+ sites cannot be equivalent. On the other hand, the **G** form does possess one trigonal planar, three-coordinate AgS_3 environment as depicted in Chart 2. The other environment is also three-coordinate, but distorted. Chart 4 shows a distorted lattice that still has half the Ag^+ in trigonal planar sites. For the **T** form, the lattice presumably deviates to an even greater extent than the structure shown in Chart 4. Another putative source of distortion in these compounds is the

Chart 4. Distorted Ag Lattice with Two Types of 3-Coordinate Ag-S Environments



possibility of increasing buckling or deformation close to the plane edges, which would also explain the noticeable lack of observation of two-coordinate edge environments in the ^{109}Ag NMR spectrum.

An interesting mechanistic issue is the impetus for **T**-**G** conversion: Is it driven by changes in Ag-S coordination chemistry, or does it cause the observed changes? A clearly attractive feature of gauche conformers, given the 50% per layer vacancy, is the increased molecular footprint in the direction of the surface normal. In other words, the gauche conformers take up more space, and that space is available because of up-down alkyl chain alteration. It is thus tempting to speculate that the tendency to fill space drives the **T**-**G** change, leading to changes in Ag-S coordination environment.

Several Raman studies of organothiolate SAMs on Ag support this notion. (i) Ag sol SERS spectra of 2×10^{-4} M solutions of 1-butanethiol show only the trans configuration for adsorbed butanethiolate, but at 5×10^{-6} M concentrations, a roughly 1:1 trans:gauche mixture of conformers is observed.^{31c} (ii) A similar phenomenon obtained for adsorbed 1-propanethiol on Ag sols;^{29a} moreover, from a plot of gauche:trans ratio vs solution concentration, it was suggested that the onset of appearance of gauche C(1)-C(2) bonds coincided with less-than-full monolayer coverage. (iii) The C-S stretch of 1-hexadecanethiol adsorbed to Ag island films exhibited a 20 cm^{-1} shift to lower frequencies with decreasing solution concentration.³⁰ The common conclusion reached by these studies is that gauche C(1)-C(2) conformers are preferred at low coverages of adsorbed thiolate. Note that while the crudely estimated activation energy for formation of **G** ($\approx 60 \text{ kJ/mol}$) is higher

than the calculated trans-gauche rotational barrier of 21 kJ/mol for the C(1)–C(2) bond of 1-propanethiol,³³ it is still quite accessible at room temperature.

Conversion of **T** to **G** leads to an increase in interlayer spacing of 1.32 Å, as measured by XRD. How can this be understood, given the decreased span of the gauche conformer? There are three feasible explanations. (i) Dance et al. claim the alkyl chains in AgS(CH₂)₃CH₃ extend perpendicular to the Ag⁺ plane. This argument is based in part on incorrect values for van der Waals radii,^{34,35} meaning the alkyl groups could actually be tilted. Indeed, if the alkyl chains are tilted at approximately 30° relative to the surface normal, the gauche conformation is actually slightly longer than the fully extended conformation. This can be easily seen with the use of CPK models (Supporting Information). (ii) According to Dance, the thickness of the Ag–S slab is 1.0–1.5 Å.¹ However, a plot of observed interlayer spacing vs alkyl chain length (from the data in that paper) shows an intercept of 0.9 Å (Supporting Information). While this value does show that the Ag–S slab is not planar, it certainly allows for an increase in slab thickness in the gauche form, given that the Ag–S covalent bond length is 2.37 Å for linear digonal coordination and 2.55 Å for trigonal coordination. Thus, slight differences in interlayer spacing can be accounted for by minor increases in slab thickness associated with changes in coordination geometry. (iii) The head group interpenetration thought to be present in all-trans AgSR (Chart 1) is sterically less favorable for the gauche form. The extent of alkyl chain interdigitation is not measured but rather calculated from the observed interlayer spacing, the alkyl chain length, and the slab thickness. Since values for the last two parameters are uncertain, the actual amount of chain interpenetration in the all-trans form is not known, but this mechanism should be less important for **G**, leading to increased layer spacing. At present, the individual effects of alkyl chain tilt, slab thickness, and chain interpenetration cannot be distinguished.

The reconstruction of Ag surfaces upon exposure to S-containing species is well-appreciated.^{5,6,11} The 3-D structure and structural transformations of AgS(CH₂)₃CH₃ are consistent with previously described findings along these lines in 2-D structures. For example, like organothiol SAMs on Ag, the **G** form has an S–S spacing of 4.42 Å, a byproduct of 2.55 Å Ag–S bonds and 120° bond angles. Even the more distorted **T** form exhibits such a spacing, as well as longer, 4.8 Å, S–S distances. The Ag⁺–thiolate coordination environment in AgS(CH₂)₃CH₃ is thus a good model for the extreme limit of surface reconstruction, i.e. literally pulling Ag⁺ ions off the surface to make Ag thiolate complexes.

The results reported herein are also significant for the liquid-crystal behavior of AgSR compounds. The yellow color that accompanies the melting of the long-chain alkyl compounds has a molecular origin, namely the change of Ag⁺ coordination environment associated with formation of gauche C(1)–C(2) conformers. The lack of covalent bonding between layers leads

to significant structural changes upon melting. However, it is unlikely that these structural changes result from decreased S bridging:² ¹⁰⁹Ag NMR clearly shows that each Ag⁺ ion in gauche AgS(CH₂)₃CH₃ is three-coordinate, necessitating triply bridging S as well. This conclusion is supported by the color change from white to yellow that is known to be associated with an increase in coordination number rather than a decrease.^{15,23}

The stability of the layered form of the **G** isomer suggests β-substituted alkyls may be capable of forming liquid-crystalline layered structures and SAMs. For example, 2-methyl-2-butanethiol has an all-trans carbon backbone and a permanent gauche interaction with the methyl group; the Ag⁺ complex should form a single phase that is yellow. SAMs with substituted and/or heteroatom-containing alkanethiols were recently described.³⁶ If such a SAM did form, wavelength-dependent in-situ ellipsometry (i.e. 300–500 nm) may give rise to resonant signal enhancement from ligand-to-metal charge transfer transitions.³⁷

Summary

Raman, X-ray diffraction, UV–visible reflectance, and ¹³C and ¹⁰⁹Ag CPMAS NMR have been used to detect and understand structural changes associated with a C(1)–C(2) trans to gauche isomerization in AgS(CH₂)₃CH₃, a layered solid. This transformation, which is accompanied by a color change from white to bright yellow, leads to an increase in interlayer spacing but not to a decrease in Ag⁺ coordination number. The S–S spacing in 3-D Ag(SCH₂)₃CH₃, derived from ¹⁰⁹Ag NMR data and crystallographically-known Ag–SR bond lengths, is very similar to that observed in closed-packed 2-D organothiol SAMs on Ag, even though the thiol occupancy in the 3-D material is only 50% that in the SAM.

Acknowledgment. We acknowledge partial support of this work from the Beckman Foundation and from the National Science Foundation (Grants CHE-9256692 and CHE-9307485). We thank Skip Knoble for assistance in rewriting the program written by Berger for use on the PSU mainframe; the Allara group for use of the temperature-controlled Raman cell; Dr. Alan Benesi for acquiring the program HBLSQFIT v4.0a by A. Kentgens, used for Herzfeld–Berger analysis, and for many useful discussions on NMR; Tom Mallouk for the use of CPK models; Tracy Oriskovich for initial experiments in this area; Perkin–Elmer for a loan of diffuse reflectance accessories; and Gerald Johnson for assistance in interpretation of XRD data and use of the Visser-ITO indexing program, Versions 13 and 15, applied in the attempted solution of the unit cell dimensions.

Supporting Information Available: An Arrhenius plot for conversion of **T** to **G**, a plot of interlayer spacing in AgS(CH₂)₃CH₃ vs the number of methylenes in the alkyl chain, and photographs of CPK models of **G** and **T** forms of S(CH₂)₃CH₃ groups at 30 and 0° tilts to the surface normal are available on the Internet only. Access information is given on any current masthead page.

IC961268N

- (33) Allinger, N. L.; Hickey, M. J. *J. Am. Chem. Soc.* **1975**, *97*, 5167–5177.
 (34) Dance et al. used the following van der Waals radii: CH₃ = 1.69 Å and H = 1.00 Å. In fact, C = 1.70 Å, H = 1.22 Å, S = 1.80 Å, and CH₃ = 2.0 Å.³⁵
 (35) (a) Douglas, B. E.; McDaniel, D. H.; Alexander, J. J. *Concepts and Models of Inorganic Chemistry*, 3rd ed.; John Wiley and Sons: New York, 1994; p 102. (b) Streitwieser, A., Jr.; Heathcock, C. H. *Introduction to Organic Chemistry*; Macmillan Publishing Co.: New York, 1976; pp 96–97.

- (36) (a) Laibinis, P. E.; Bain, C. D.; Nuzzo, R. G.; Whitesides, G. M. *J. Phys. Chem.* **1995**, *99*, 7663–7676. (b) Chang, S.-C.; Chao, I.; Tao, Y.-T. *J. Am. Chem. Soc.* **1994**, *116*, 6792–6805. (c) Evans, S. D.; Freeman, T. L.; Flynn, T. M.; Batchelder, D. N.; Ulman, A. *Thin Solid Films* **1994**, *244*, 778–783.
 (37) An interesting, recent ellipsometric study on Langmuir monolayers of silver *n*-octadecanethiolate has appeared (Zhao, W.; Kim, M. W.; Wurm, D. B.; Brittain, S. T.; Kim, Y.-T. *Langmuir* **1996**, *12*, 386–3910), but it employed a 632.8-nm light source.